HAL open science

A novel approach to the synthesis of unsupported nickel phosphide catalysts using nickel thiophosphate as precursor

Hermione Loboué, Catherine Guillot-Deudon, Aurelian Florin Popa, Alain Lafond, Bernadette Rebours, Christophe Pichon, Tivadar Cseri, Gilles Berhault, Christophe Geantet

To cite this version:

Hermione Loboué, Catherine Guillot-Deudon, Aurelian Florin Popa, Alain Lafond, Bernadette Rebours, et al.. A novel approach to the synthesis of unsupported nickel phosphide catalysts using nickel thiophosphate as precursor. Catalysis Today, 2008, 130 (1), pp.63-68. 10.1016/j.cattod.2007.07.005 . hal-00283610

HAL Id: hal-00283610

https://hal.science/hal-00283610v1

Submitted on 29 Sep 2022

HAL is a multi-disciplinary open access archive for the deposit and dissemination of scientific research documents, whether they are published or not. The documents may come from teaching and research institutions in France or abroad, or from public or private research centers.

L'archive ouverte pluridisciplinaire **HAL**, est destinée au dépôt et à la diffusion de documents scientifiques de niveau recherche, publiés ou non, émanant des établissements d'enseignement et de recherche français ou étrangers, des laboratoires publics ou privés.

Distributed under a Creative Commons Attribution - NonCommercial 4.0 International License

A novel approach to the synthesis of unsupported nickel phosphide catalysts using nickel thiophosphate as precursor

Hermione Loboué [a], Catherine Guillot-Deudon [b], Aurelian Florin Popa [b], Alain Lafond [b], Bernadette Rebours [c], Christophe Pichon [c], Tivadar Cseri [c], Gilles Berhault [a,*], Christophe Geantet [a]

[a] *Institut de Recherches sur la Catalyse et l'Environnement de Lyon, IRCELYON, UMR 5256 CNRS, Université Lyon I, 2 Avenue Albert Einstein, 69626 Villeurbanne Cedex, France*

[b] *Institut des Matériaux Jean Rouxel, IMN, UMR 6502 CNRS, Université de Nantes, 2 rue de la Houssinière, Nantes F-44322, France*

[c] *IFP, IFP-Lyon, BP 3, 69390 Vernaison, France*

Nickel thiophosphate, $NiPS_3$ synthesized at room temperature using a soft chemistry approach (a-$NiPS_3$) has been successfully used as precursor for low-temperature preparation of unsupported nickel phosphide. Using Raman spectroscopy and EXAFS, comparison with a well-crystallized $NiPS_3$ reference (c-$NiPS_3$) first confirmed that nickel thiophosphate can be effectively obtained at low temperatures of preparation. In situ XRD diffraction and EXAFS showed that Ni_2P was obtained by the reduction of a-$NiPS_3$ at a temperature as low as 573 K. For c-$NiPS_3$, slower kinetics of reduction first led to the formation of an intermediate richer phosphorus-containing nickel phosphide phase, Ni_5P_4 at a temperature of reduction of 623 K while Ni_2P started being formed at 773 K. Under hydrodesulfurization (HDS) thiophene catalytic conditions (613 K, 2.8 mol% thiophene/H_2), a-$NiPS_3$ was decomposed into a mixture of Ni_2P and Ni_5P_4 while c-$NiPS_3$ was converted into Ni_5P_4. Both nickel phosphide catalysts exhibit much higher activities compared to a MoS_2 reference. Ni_5P_4 exhibited a specific activity (per gram of catalyst) seven times as high as for MoS_2.

Keywords: Hydrodesulfurization; $NiPS_3$; Nickel phosphide; Soft chemistry

1. Introduction

The decreasing quality of petroleum feedstock and the drastic environmental regulations have triggered studies to improve the efficiency of hydrotreating processes. One solution to achieve this goal is to develop new catalytic systems other than the traditional MoS_2-based catalysts. In the last years, a new class of materials, the transition metal phosphides (i.e. MoP, WP, Ni_2P) have been found quite promising as alternative hydrodesulfurization (HDS) catalysts [1–3]. In particular, Oyama et al. observed that Ni_2P/SiO_2 was more active than the conventional $NiMo/Al_2O_3$ and $CoMo/Al_2O_3$ catalysts for the HDS of dibenzothiophene [2]. They also proposed that the surface active phase was in fact a nickel phosphosulfide [4,5].

Transition metal phosphides are generally prepared by the reduction of phosphate-containing precursors at high temperature (853–923 K) [1,6–8]. This high reducing treatment is required due to the P–O bond strength. However, such a procedure of preparation limits the use of nickel phosphide as relevant alternative to $CoMo/Al_2O_3$ or $NiMo/Al_2O_3$ as HDS catalysts. Therefore, other methods of preparation using lower temperatures of treatment are strongly needed in order to develop highly active Ni_2P-based HDS catalysts. In this respect, Liu et al. synthesized unsupported Ni_2P in the presence of polyacrylamide under mild conditions (453 K) using solvothermal techniques [9]. However, even if successful, this technique cannot be used for preparing silica-supported catalysts. Similarly, Yang et al. proposed the use of the hazardous PH_3/H_2 reactant mixture for preparing Ni_2P from Ni metal particles [10].

Another alternative would be to use precursors with P–S bonds easier to break than the P–O bonds. In this respect, Robinson et al. used nickel thiophosphate, $NiPS_3$ in the

* Corresponding author. Tel.: +33 472 44 53 20; fax: +33 472 44 53 99.
E-mail address: Gilles.Berhault@ircelyon.univ-lyon1.fr (G. Berhault).

hydrodenitrogenation (HDN) of quinoline and observed its decomposition into Ni_2P after a H_2S/H_2 (10%, v/v, H_2S) treatment at 15 bars and 643 K [11]. Similarly, Koranyi observed the transformation of $NiPS_3$ into Ni_2P at 923 K under atmospheric pressure [12]. However, $NiPS_3$ was prepared in these studies at high temperature (973 K) from elementary elements in a sealed tube using solid-state techniques.

Prouzet et al. were able to synthesize $NiPS_3$ in a poorly crystalline state through the reaction of $NiCl_2$ and Li_2PS_3 at room temperature [13]. In the present study, this soft chemistry route was used to prepare unsupported $NiPS_3$ catalysts that can be decomposed at low temperature into highly active HDS nickel phosphide catalysts.

2. Experimental

2.1. Synthesis of the unsupported nickel thiophosphates

Two forms of $NiPS_3$ were prepared: crystalline $NiPS_3$ (c-$NiPS_3$) was obtained by a solid-state reaction route while amorphous $NiPS_3$ (a-$NiPS_3$) was synthesized by soft chemistry route.

For the preparation of c-$NiPS_3$, a mixture of powdered Ni, P and S flakes, weighed in the proportion 1:1:3 in a dry-box was sealed in a silica tube under vacuum and heated at 973 K for 48 h. A polycrystalline sample was obtained. Elemental analysis revealed a final stoichiometry, $NiPS_{2.8}$. The BET specific surface area was 1 m^2/g.

The preparation at room temperature of a-$NiPS_3$ was adapted from the soft chemistry process previously described by Prouzet et al. [13]. To avoid contamination of catalysts by chloride anion, we used nickel nitrate as nickel precursor. In a typical procedure, 30 mL of an aqueous solution of nickel nitrate ($Ni(NO_3)_2{\cdot}6H_2O$) of 0.36 M was added drop by drop to 50 mL of an aqueous Li_2PS_3 solution (0.43 M) under a vigorous stirring and a N_2 gas flux. The resulting red gel was centrifuged and then washed with water three times successively. The compound was finally dried under vacuum in an oven during one night. The precursor Li_2PS_3 was prepared in powder form by solid-state reaction at 723 K for 48 h. The XRD pattern revealed the presence of $Li_4P_2O_7$ as impurity, which is fortunately insoluble in aqueous media. Elemental analysis revealed a final stoichiometry $NiPS_{2.9}$. The BET specific surface area was 1 m^2/g.

2.2. Catalyst characterization

Surface area was determined by N_2 adsorption at 77 K using BET equation on a home-made apparatus after degassing the catalyst samples at 673 K during 2 h. Raman spectra were recorded with a Raman Jobin Yvon, Labram HR800 spectrometer. The 514.53 nm exciting wavelength of an argon–krypton laser was focused using a 50× objective. The laser power on the samples was typically 4 mW. Wavenumbers measurements were accurate within ca. 3 cm^{-1}. In situ X-ray diffraction measurements were performed on a Panalytical X'Pert Pro θ/θ diffractometer equipped with a curved graphite monochromator using Cu Kα radiation. The reaction cell (XRK 900 Anton Paar) was equipped with an open holder allowing gas to pass through the sample. H_2 flow was adjusted at 1 L/h. Temperature-programmed reduction was as follows—heating ramp: 10 K/min from RT to 973 K with 45 min plateaus each 50 K. Before acquisition, samples were maintained 15 min at each temperature plateau (acquisition time: 30 min). The diffractograms were analyzed using the standard JCPDS files.

EXAFS experiments were carried out at the X1 beam line of the HASYLAB facility (Hamburg, Germany) using the synchrotron radiation from the DORIS III ring running at 4.45 GeV (with positrons) with an average current of 120 mA. The Ni K edge at 8333 eV was monitored in the transmission mode with three ion chambers as detectors (measuring intensity before and after the sample and a metallic Ni foil reference). The signal-to-noise ratio was optimised by acquiring multiple scans for each spectrum. To characterize the Ni environment evolution during reduction treatments, a dedicated cell for in situ measurements was used [14]. EXAFS analysis was performed using the Athena-Artemis software package [15]. EXAFS data analysis was performed using theoretical back-scattering phases and amplitudes calculated with FEFF6 code [16]. Since a very accurate structural model was necessary to analyze the EXAFS data, the $NiPS_3$ structure was reinvestigated. The interatomic distances deduced from this structural study were referred as "standard references".

2.3. Thiophene HDS catalytic measurements

The thiophene HDS test was carried out in an open microreactor at atmospheric pressure. The $NiPS_3$ samples were directly transferred to the HDS reactor without any pretreatment. The intrinsic activities were examined at 573 K using a 2.8 mol% thiophene feed in hydrogen. In a typical experiment, 50 mg of catalyst powder was placed into the reactor leading to a bed dimension of 12 mm × 2.5 mm. Conversions were kept in the range 10–15% in order to avoid mass transfer limitations. Under these conditions, the H_2S concentration produced by the reaction never exceeds 2000 ppm. The rate of the reaction was determined under steady-state conditions and expressed as:

$$r = \frac{F_0}{wS} x \, (\mathrm{mol}/(\mathrm{m}^2\,\mathrm{s})),$$

where x is conversion, w the mass of the catalyst (g), S the BET specific surface area of the catalyst after their decomposition into phosphide and F_0 is the molar flow of the reactant (mol/s). The specific activity will refer to the number of molecules of reactant converted per second and per gram of catalyst while the intrinsic activity will correspond to the number of molecules of reactant per second and per m^2.

3. Results and discussion

3.1. Characterization by XRD, EXAFS and Raman spectroscopy

In a first step, the nickel thiophosphate obtained using soft chemistry techniques, a-$NiPS_3$ was characterized and com-

Table 1
EXAFS curve-fitting results for c-$NiPS_3$ and a-$NiPS_3$

	Ni–S	Ni–Ni	Ni–P
Standard reference parameters[a]			
R (Å)	2.4676(4)	3.3593(2)	3.5277(3)
	2.4646(4)	3.3675(4)	3.5288(5)
	2.4634(4)		3.5379(4)
CN	2	2	2
	2	1	2
	2		2
c-$NiPS_3$			
R (Å)	2.46	3.34	3.57
ΔE_0 (eV)	3.8	–	–
CN	6[b]	3	6
σ^2 (Å^2)	0.0080	0.0082	0.0066
a-$NiPS_3$			
R (Å)	2.46	3.37	3.60
ΔE_0 (eV)	4.1	–	–
CN	4.9	2.8	3.7
σ^2 (Å^2)	0.0106	0.0129	0.0170

[a] From single crystal structure refinement [results to be published].
[b] Value fixed at 6, $s_0^2 = 0.73$.

pared to the reference crystalline sample, c-$NiPS_3$. Fig. 1 reports the Fourier transforms of the EXAFS spectra at the Ni K edge for both a-$NiPS_3$ and c-$NiPS_3$. The Fourier transforms for both samples gave two similar peaks, the first one corresponding to the Ni–S shell and the second one to the Ni–Ni and Ni–P shells. Table 1 gives the standard crystallographic data for $NiPS_3$ and the curve-fitting results of the EXAFS spectra for both c-$NiPS_3$ and a-$NiPS_3$. For c-$NiPS_3$, distances for the Ni–S and Ni–Ni shells were in very good agreement with standard data while slightly longer distances were found for the Ni–P shell. For a-$NiPS_3$, a quite good agreement was also observed for the Ni–S and Ni–Ni shells while the Ni–P distance appeared once again longer than for c-$NiPS_3$ and the standard reference. In the a-$NiPS_3$ compound, coordination numbers for the Ni–P shell decreased compared to the well-crystallized c-$NiPS_3$ confirming a less ordered structure at long distance.

Raman studies were performed to confirm the assignment of the compound synthesized using low-temperature techniques. Fig. 2 reports the Raman spectra of both a-$NiPS_3$ and c-$NiPS_3$ while Table 2 summarizes the different Raman frequencies detected on the two samples and their corresponding modes of vibration according to the study of Mathey et al. [17]. Both samples present three similar groups of Raman bands in the 700–150 cm^{-1} wavenumbers range [17,18]. However, while the $T'_{xy}(PS_3)$ vibration was observed in both cases at 185 cm^{-1}, the symmetric stretching vibration of the PS_3 group shifted by 14 cm^{-1} to lower wavenumbers from 392 to 378 cm^{-1} for a-$NiPS_3$ compared to the c-$NiPS_3$ reference. The doubly-degenerate $\nu_d(PS_3)$ bands shifted only by 2–4 cm^{-1} from 567 to 565 cm^{-1} and from 596 to 592 cm^{-1}. This would suggest a slightly different P–S bond length in the a-$NiPS_3$ compound.

3.2. *In situ reduction of a-$NiPS_3$ and c-$NiPS_3$ into nickel phosphides*

3.2.1. *In situ XRD study*

The reduction of the two different $NiPS_3$ precursors was followed using in situ X-ray diffraction to determine the process of decomposition of nickel thiophosphate into nickel phosphide. Fig. 3A reports the evolution of the XRD patterns of c-$NiPS_3$ during the H_2 reduction of this well-crystallized nickel thiophosphate compound from RT to 873 K. The $NiPS_3$ initial structure was characterized mainly by the intense (0 0 1) peak at $2\theta = 14.0°$. Other $NiPS_3$ peaks (JCPDS file 01-078-0499) were observed in the 28–58° 2θ range. Up to 573 K, the $NiPS_3$ structure was preserved. At 623 K, new peaks were detected at 40.4°, 43.9°, 46.6° and 53.9° corresponding, respectively, to the (2 1 0), (2 1 2), (3 0 1) and (2 2 0) reflections of the Ni_5P_4 phase (JCPDS 00-018-0883). At 673 K, all the diffraction peaks between $2\theta = 28.0°$ and 54° were assigned to the Ni_5P_4 phosphide while only weaker diffraction peaks of $NiPS_3$ were still observed. At 723 K, only the Ni_5P_4 phase was detected. At 773 K, new diffraction peaks were observed at $2\theta = 40.4°$,

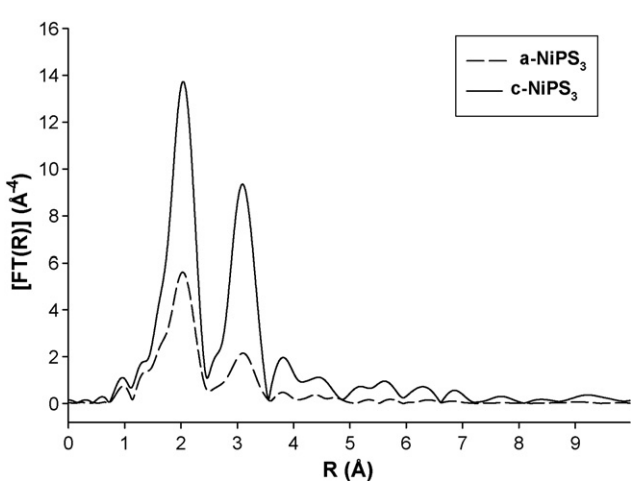

Fig. 1. Fourier transforms of the EXAFS spectra at the Ni K edge of the well-crystallized c-$NiPS_3$ and a-$NiPS_3$ synthesized at low temperature.

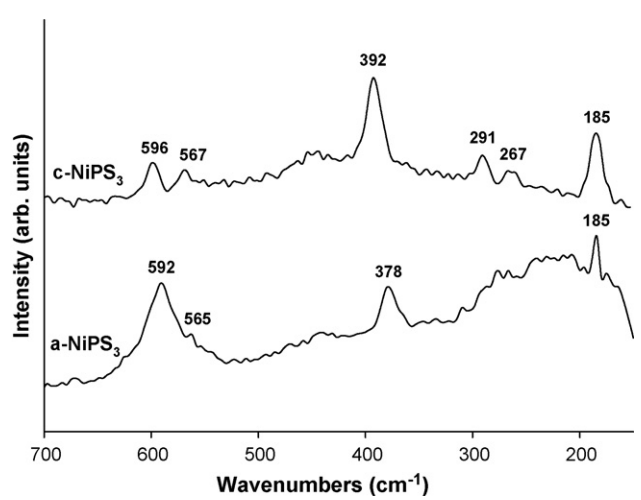

Fig. 2. Raman spectra of the well-crystallized c-$NiPS_3$ and a-$NiPS_3$ synthesized at low temperature.

Table 2
Attribution of the different Raman frequencies of the two $NiPS_3$ samples: a-$NiPS_3$ obtained by soft chemistry approach, and c-$NiPS_3$ obtained at high temperature using solid-state techniques

Raman frequencies (cm^{-1})		Modes of Vibration[1]	Symmetry
c-$NiPS_3$	a-$NiPS_3$		
185	185	$T''_{xy}(PS_3)$	E_g
267	/	$T''_{xy}(PS_3)$	E_g
291	/	$\delta_d(PS_3)$	E_g
392	378	$\nu_s(PS_3)$	A_{1g}
567	565	$\nu_d(PS_3)$	E_g
596	592	}	

[1]According to Ref. [18].

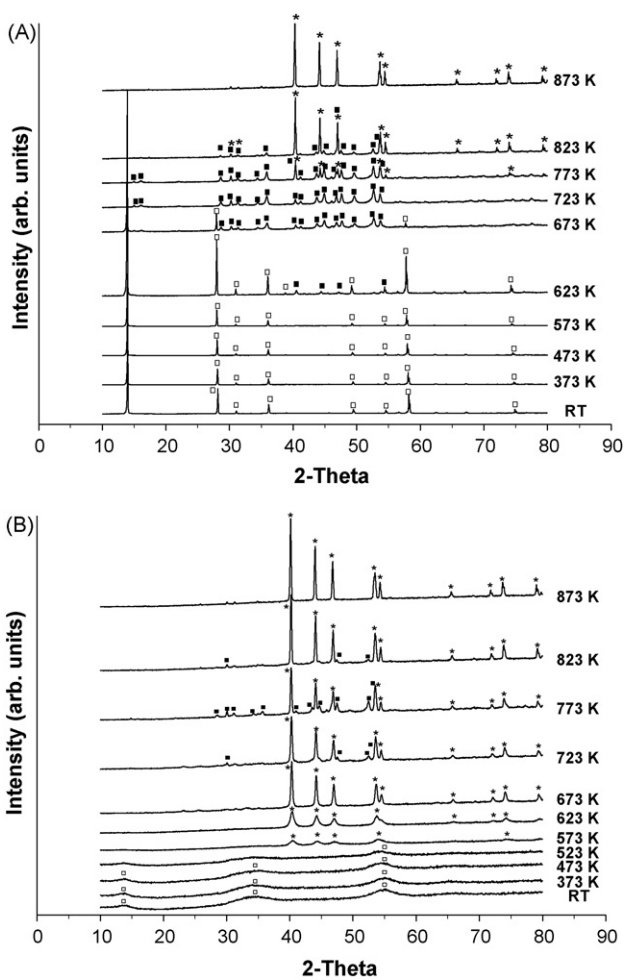

Fig. 3. Evolution of the XRD patterns of (A) c-$NiPS_3$ and (B) a-$NiPS_3$ during their in situ reduction into nickel phosphide (symbols: □, $NiPS_3$; ■, Ni_5P_4; *, Ni_2P).

44.2°, 47.0°, 53.5°, 54.5° and 74.0° corresponding, respectively, to the most intense (1 1 1), (2 0 1), (2 1 0), (3 0 0) + (0 0 2), (2 1 1) and (4 0 0) + (2 1 2) reflections of the Ni_2P phase (JCPDS 01-089-2742). At 823 K, the diffraction peaks corresponding to the Ni_2P phase became more intense while weaker reflections were still visible for the Ni_5P_4 phase. At 873 K, only intense diffraction peaks corresponding to Ni_2P were observed.

Therefore, the decomposition of c-$NiPS_3$ into phosphide started at 623 K. This decomposition occurred through the formation of an intermediate Ni_5P_4 phosphide phase. Ni_5P_4 is the only phosphide phase observed at a reduction temperature of 723 K while Ni_2P started being observed at 773 K. Ni_2P was the only phosphide phase after reduction at 873 K. The formation of the intermediate richer phosphorus-containing Ni_5P_4 (P/Ni = 0.8) indicates a slow kinetics of reduction of nickel thiophosphate $NiPS_3$ (P/Ni = 1) into dinickel phosphide, Ni_2P (P/Ni = 0.5) and therefore a progressive decrease of the phosphorus content during the reduction process [6].

In situ X-ray diffraction studies were also carried out during the reduction of the nickel thiophosphate compound, a-$NiPS_3$, synthesized at low temperature (Fig. 3B). a-$NiPS_3$ was detected up to a temperature of reduction of 523 K. Ni_2P was formed as low as 573 K. Ni_5P_4 was temporarily observed between 723 and 823 K. However, contrary to c-$NiPS_3$, Ni_5P_4 was never the only nickel phosphide phase detected. Diffraction peaks of Ni_2P were detected all along the 573–873 K temperature range. At 873 K, once again, Ni_2P was the only nickel phosphide phase observed. Results suggest a faster kinetics of reduction for a-$NiPS_3$ compared to c-$NiPS_3$ since Ni_2P was detected already at 573 K vs. 773 K for c-$NiPS_3$. Since the main difference between the two nickel thiophosphate compounds is the crystallite size of the $NiPS_3$ particles, this would suggest that the release of phosphorus as PH_3 during the reduction of $NiPS_3$ into Ni_2P (about 50% of the amount initially present in Ni_5P_4) on small crystallites is too fast. In that case, this would not allow the formation of the intermediate richer phosphorus nickel phosphide Ni_5P_4 phase (obtained by elimination of 20% of P initially present in $NiPS_3$). In that case, Ni_5P_4 detected between 723 and 823 K would then result from the initial presence of some bigger crystallites of $NiPS_3$ for which the slower kinetics of reduction would allow the intermediate formation of this rich phosphorus-containing nickel phosphide. Therefore, a certain degree of heterogeneity in the initial particle size distribution of a-$NiPS_3$ was expected. These results emphasize the interest of the low-temperature synthesis of $NiPS_3$ since Ni_2P was obtained at a much lower temperature than for the well-crystallized c-$NiPS_3$ (573 K vs. 773 K).

3.2.2. *EXAFS study*

The reduction of the a-$NiPS_3$ precursor was also followed using EXAFS at the Ni K edge (Fig. 4). Results showed that the Fourier transform of a-$NiPS_3$ reduced at 473 K was quite similar to the non-reduced sample confirming that at this temperature of reduction, the $NiPS_3$ structure was preserved. Only a slight shift to lower distance could be detected for the first Ni–S shell [19]. At a temperature of reduction of 573 K, the

Table 3
BET surface areas (before and after HDS test), nature of the final active phase (determined by XRD), specific and intrinsic activity results of the different unsupported nickel thiophosphate compounds, a-$NiPS_3$ and c-$NiPS_3$ directly used in the HDS of thiophene at 613 K (2.8 mol% thiophene/H_2)

Samples	Initial surface area (m^2/g)	Nature of the final active phase	Specific activity (10^{-7} mol/(g_{cat} s))	Intrinsic activity (10^{-8} mol/(m^2 s))	Final surface area (m^2/g)
a-$NiPS_3$	1	Ni_5P_4 + Ni_2P	9.0	4.3	21
c-$NiPS_3$	1	Ni_5P_4	14.7	4.9	30
MoS_2	18	–	2.2	1.2	–

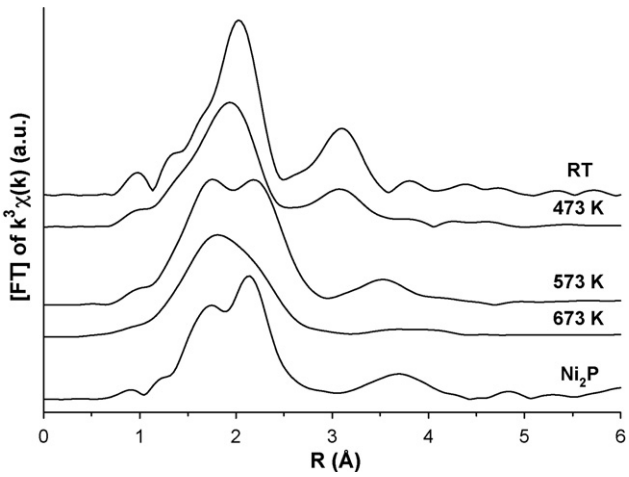

Fig. 4. Evolution of the Fourier transforms of the EXAFS spectra at the Ni K edge during the reduction of a-$NiPS_3$ synthesized at low temperature.

peak profiles changed dramatically. Two new features appeared in the first envelope at lower and higher values than those previously found for Ni–S distances of a-$NiPS_3$. Comparison with a Ni_2P reference showed that these two prominent peaks correspond, respectively, to the Ni–P and Ni–Ni shells of bulk Ni_2P even if the Ni–Ni distance were slightly longer for the sample reduced at 573 K. At 673 K, the peaks profile broadened. This could result from the appearance of a Ni–S contribution at about 2.0 Å as already observed for partially surface sulfided Ni_2P [6]. This may be expected since $NiPS_3$ during its reduction into Ni_2P very probably lost sulfur as H_2S. This sulfur loss should represent 50% of its initial weight. Therefore, the in situ EXAFS study confirmed that Ni_2P was obtained as low as a temperature of reduction of 573 K as already observed before using in situ XRD.

3.3. HDS catalytic activity

Table 3 summarizes the intrinsic activity for the HDS of thiophene of the two different $NiPS_3$ samples and of a MoS_2 reference [20]. The c-$NiPS_3$ sample exhibited strong but slow activation phenomenon (not shown here) during the first 20 h of time-on-stream revealing a modification of the nature of the active phase under the HDS conditions. XRD characterization of the catalyst after the catalytic test confirmed this fact revealing the formation of Ni_5P_4. This result is consistent with the in situ XRD study presented above. Indeed, at a temperature of reduction of 623 K, Ni_5P_4 was already detected during the reduction of c-$NiPS_3$. It should also be noted that the remaining $NiPS_3$ phase was almost undetected on the sample after the HDS test while still strong $NiPS_3$ diffraction peaks were found during the in situ XRD study. Since the XRD test was performed after one day under catalytic conditions, this result confirms a slow kinetic transformation of c-$NiPS_3$ into Ni_5P_4. Moreover, elemental analysis after HDS test corresponds to a final $Ni_{5.0}P_{4.2}S_{0.1}$ stoichiometry. This result showed that (1) Ni_5P_4 was probably the only nickel phosphide phase formed and (2) that 95% of sulfur was lost during the course of the HDS run while only 20% of phosphorus was removed.

For a-$NiPS_3$, a similar activation phenomenon was observed. However, steady-state conditions were achieved faster (after 7 h of time-on-stream). XRD characterization after test also showed a modification of the active phase during the catalytic test revealing the presence of intense peaks of Ni_2P but also weaker peaks of Ni_5P_4. The elemental analysis after test showed a final $Ni_{5.0}P_{4.3}S_{<0.1}$ stoichiometry. Therefore, the intense XRD peaks of Ni_2P correspond to a minority of big crystalline Ni_2P particles while the vast majority of the active phase consists into Ni_5P_4 particles. This decomposition of both $NiPS_3$ samples during the thiophene HDS test also led to a strong increase of the surface area: from 1 to 21 m^2/g for a-$NiPS_3$ and for 1 to 30 m^2/g for c-$NiPS_3$ (Table 3). Comparison with a MoS_2 reference showed that both catalysts present better specific (or intrinsic) HDS activity. In terms of specific activity, unsupported Ni_5P_4 resulting from the decomposition of c-$NiPS_3$ is seven times more active than MoS_2. If activities are compared on per specific surface area (intrinsic activity), results are still favourable for the nickel phosphide catalysts. In this case, nickel phosphides present similar intrinsic activities which are four times as high as for MoS_2.

4. Conclusion

Nickel thiophosphate, $NiPS_3$, was synthesized at low temperature using a soft chemistry route. This compound was used in the present study as a new precursor of nickel phosphide catalysts. In a first part, comparison with a well-crystallized $NiPS_3$ reference confirmed that the nickel thiophosphate phase was obtained using our low-temperature method of preparation. In situ XRD studies of the reduction of $NiPS_3$ showed that slow kinetics of reduction led to the formation of the intermediate richer phosphorus-containing Ni_5P_4 phase. Moreover, Ni_2P was obtained from $NiPS_3$ at a reduction temperature as low as 573 K. Finally, compared to MoS_2, thiophene HDS results showed superior activities of the two nickel phosphide catalysts particularly for Ni_5P_4.

Acknowledgements

H. Loboué thanks IFP and SIR (Société Ivoirienne de Raffinage) for their financial support.

References

[1] X. Wang, P. Clark, S.T. Oyama, J. Catal. 208 (2002) 321.
[2] S.T. Oyama, J. Catal. 216 (2003) 343.
[3] S.J. Sawhill, D.C. Phillips, M.E. Bussell, J. Catal. 215 (2003) 208.
[4] S.T. Oyama, X. Wang, Y.K. Lee, W.J. Chun, J. Catal. 221 (2004) 263.
[5] T. Kawai, K.K. Bando, Y.K. Lee, S.T. Oyama, W.J. Chun, K. Asakura, J. Catal. 241 (2006) 20.
[6] S.T. Oyama, X. Wang, Y.K. Lee, K. Bando, F.G. Requejo, J. Catal. 210 (2002) 207.
[7] J.A. Rodriguez, J.Y. Kim, J.C. Hanson, S.J. Sawhill, M.E. Bussell, J. Phys. Chem. B 107 (2003) 6276.
[8] V. Zuzaniuk, R. Prins, J. Catal. 219 (2003) 85.
[9] J. Liu, X. Chen, M. Shao, C. An, W. Yu, Y. Qian, J. Cryst. Growth 252 (2003) 297.
[10] S. Yang, C. Liang, R. Prins, J. Catal. 237 (2006) 118.
[11] W.R.A.M. Robinson, J.N.M. van Gestel, T.I. Koranyi, S. Eijsbouts, A.M. van der Kraan, J.A.R. van Veen, V.H.J. de Beer, J. Catal. 161 (1996) 539.
[12] T.I. Koranyi, Appl. Catal. A: Gen. 239 (2003) 253.
[13] E. Prouzet, G. Ouvrard, R. Brec, P. Seguineau, Solid State Ionics 31 (1988) 79.
[14] C. Geantet, Y. Soldo, C. Glasson, N. Matsubayashi, M. Lacroix, O. Proux, O. Ulrich, J.-L. Hazemann, Catal. Lett. 73 (2001) 95.
[15] B. Ravel, M. Newville, J. Synch. Rad. 12 (2005) 537.
[16] J.J. Rehr, R.C. Albers, Rev. Mod. Phys. 72 (2000) 621.
[17] Y. Mathey, R. Clement, C. Sourisseau, G. Lucazeau, Inorg. Chem. 19 (1980) 2773.
[18] C. Sourisseau, Y. Mathey, I. Kerrache, C. Julien, J. Raman Spectrosc. 27 (1996) 303.
[19] G. Ouvrard, E. Prouzet, R. Brec, S. Benazeth, H. Dexpert, J. Chim. Phys. 86 (1989) 1675.
[20] J.A. De Los Reyes, M. Vrinat, C. Geantet, M. Breysse, J. Grimblot, J. Catal. 142 (1993) 455.